Contents list available at CBIORE journal website

International Journal of Renewable Energy Development

Journal homepage: https://ijred.cbiore.id

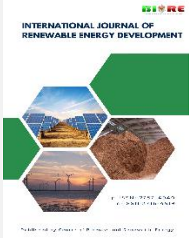

/Research Article

Advanced composite adsorbent based on biochar, bentonite, and boric acid for sustainable removal of Pinoxaden

Safa Waleed Shakir[a*] and Atheer Mohammad Al-Yaqoobi[b]

[a] *Department of Chemical Engineering, College of Engineering, University of Tikrit, Iraq.*

[b] *Department of Chemical Engineering, College of Engineering, University of Baghdad, Iraq.*

Abstract. Pinoxaden is a post-emergence herbicide, which is widely applied for the control of wheat, barley, and other cereals. Its usage is increasing across the world, and there have been concerns regarding contamination of water bodies due to residues. In this research, we investigated the removal of Pinoxaden by a new boric-acid-activated biochar–bentonite composite. The composite was synthesized by pyrolyzing biomass with boric acid and bentonite clay. The composite was studied using XRD, SEM, FTIR, and BET analysis, which showed that it has a very porous structure and boron–oxygen features on its surface. Batch adsorption experiments (pH variation, time variation, and variation of initial concentration) demonstrated rapid uptake with high capacity. Kinetic analysis was pseudo-second-order, and equilibrium data obeyed the Langmuir isotherm, indicative of monolayer chemisorption. Researchers realized maximum adsorptive capacities of 150 mg/g, within the range of 5–100 mg/g. The removal efficiency was found, through a batch adsorption study, to be a maximum of more than 99.5% at optimum conditions. Increased Pinoxaden concentration and topped-up adsorbent loading reduced the adsorptive capacity but increased with maximum adsorbent loading. The data followed the Freundlich isotherm ($R^2 > 0.999$), which shows that the adsorption happens in multiple layers, and it matched the pseudo-second-order model, indicating that the process involves chemical bonding. Studies on how substances move within particles and how they come off showed that the surface features and the movement through pores were more important than the overall amount taken in. We found that adding boric acid significantly increased the polarity and reactivity by boosting the adsorptive capacity from raw biochar or bentonite. The research shows that the MC-Db composite could be a useful, eco-friendly material that effectively removes herbicides from contaminated water.

Keywords: Pinoxaden, composite, adsorption, kinetic, adsorption isotherm

Received: 20th July 2025; Revised: 26th Sept 2025; Accepted:5th Oct 2025; Available online: 21st Oct 2025

1. Introduction

Herbicides are crucial to modern agriculture because they facilitate efficient weed control and increased crop yields. One such herbicide is Pinoxaden, a post-emergence herbicide introduced in the mid-2000s that is currently registered globally for the management of grass weeds in cereals (McManus *et al.* 2021). Despite being of moderate toxicity, Pinoxaden is soluble in water (~200 mg/L) and has been detected at trace levels in surface water and shallow groundwater based on agricultural runoff (McManus *et al..*. 2021; Andrunik *et al.* 2025). While European Union environmental monitoring suggests that Pinoxaden and its metabolites are rarely >0.1 μg/L in groundwater, runoff and irrigation ditches remain vulnerable to contamination (McManus *et al.* 2021; Andrunik *et al.* 2025). Because >20% of herbicide application rates may find their way into non-target aquatic ecosystems (Raheem *et al.* 2024; Andrunik *et al.* 2025), the long-term environmental impact of such persistent micropollutants is increasingly of concern. Conventional water treatment technologies, relying on coagulation, sedimentation, and biologic filtration, are largely ineffective on removal of such low-concentration organic contaminants. Therefore, herbicides like Pinoxaden are likely to be passed through as "micro-contaminants", persisting in treated effluents (Hassan *et al.* 2024; Raheem *et al.* 2024; Andrunik *et al.* 2025). Therefore, more sophisticated treatment technologies such as oxidation, membrane filtration, and notably adsorption have increasingly been applied owing to their higher elimination efficiency, energy conservation, and versatility towards a wide range of contaminant types (Ashiq *et al.* 2019; Abd *et al.* 2023; Blachnio *et al.* 2023; Shakir *et al.* 2025b). Among them, adsorption has been a versatile adsorbent. A wide variety of materials have been explored, including biochar, activated carbon, clays (e.g., bentonite and montmorillonite), zeolites, mesoporous silicas, and carbon nanotubes (McManus *et al.* 2021; Andrunik *et al.* 2025; Shakir *et al.* 2025b). These adsorbents possess peculiar properties: pyrolyzed agricultural waste-derived biochar is characterized with high porosity and surface functionalization potentiality; clays like bentonite possess layered structures with high cation-exchange capacity; and synthetic zeolites and mesoporous silicas can offer selective adsorption through tunable pore structures and surface chemistries (Abd *et al.* 2024; Ali *et al.* 2024; Mahmood *et al.* 2025;

---

* Corresponding author

Email: eng.safawaleed@tu.edu.iq (S.W.ShakirI

https://doi.org/10.61435/ijred.2025.61503

ISSN: 2252-4940/© 2025.The Author(s). Published by CBIORE

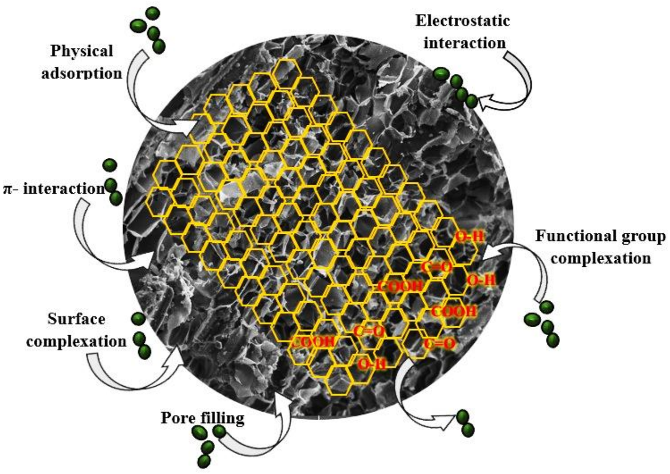

Fig 1. the possible interactions of composite with Pesticides

Shakir *et al.* 2025b). Composite materials have seen their appeal in recent years because of their synergistic adsorption behavior. For instance, a graphene oxide–silica monolith was reported to show enhanced Pinoxaden uptake through π–π stacking interactions and expanded surface area (Ali *et al.* 2024; Mahmood *et al.* 2025; Abd *et al.* 2024). Similarly, clay–biochar hybrids were reported to surpass individual components by exploiting the ion-exchange capacity of clays and surface functional chemistries of biochar (Al-Yaqoobi *et al.* 2023; Ali *et al.* 2024; Mahmood *et al.* 2025). Adsorption mechanisms for herbicides are usually intricate, involving π–π interactions, electrostatic attraction, hydrogen bonding, hydrophobic partitioning, and ion exchange (Blachnio *et al.* 2023; Shakir *et al.* 2025a). For example, carbonaceous adsorbents favor the use of π–π stacking and hydrogen bonding with aromatic herbicides, but clay minerals use ion-exchange and intercalation reactions. Figure 1 shows the possible interactions of composite with Pesticides. Notably, surface functional groups, such as hydroxyl, carbonyl, and amino groups, play a crucial role in enhancing adsorption by hydrogen bonding and acid–base interactions (Majeed *et al.* 2017; Ali *et al.* 2024). Adsorbent surface charge, pH-dependent, also dictates adsorption by electrostatic interactions. For instance, positively charged surfaces can adsorb anionic herbicide species and improve the uptake efficiency at an optimum pH value ((Majeed *et al.* 2017; Xu *et al.* 2020; Blachnio *et al.* 2023; Ali *et al.* 2024). Several studies have testified to the better performance of composite systems relative to single-component adsorbents. A municipal-waste-biochar/bentonite composite, for example, exhibited 40% greater ciprofloxacin adsorption relative to pristine biochar with a Langmuir maximum capacity of 190 mg/g (Blachnio *et al.* 2023). Likewise, boron-doped biochar, which are produced through boric acid treatment of biomass, have been found to exhibit significant enhancements in surface area and adsorption capacity. Zhang *et al.* (2022) demonstrated that boric acid treatment doubled the surface area of the biochar (up to 1190 m^2/g) as well as greatly enhanced sulfamethoxazole adsorption (Zhang *et al.* 2022). Therefore, the aim of the present study is to fabricate and evaluate a novel biochar–bentonite–boric acid composite (BBBC) for selective removal of Pinoxaden from aqueous solutions. The composite material is designed by coupling the extensive surface and π–π interaction potential of boron-doped biochar with ion-exchange and swelling of bentonite clay. By combining multiple adsorption mechanisms within a single material system, this study seeks to demonstrate the potential of BBBC as an effective adsorbent for remediating persistent herbicide.

2. Materials and Methods

2.1 Composite Synthesis

The composite was fabricated by blending MgO-catalyzed modified biochar from Dedonea biomass (MC-Db) as prepared with bentonite clay using a 1:1 mass ratio. The mixture was soaked in 0.5 M boric acid solution and left to stand for 24 hours to allow incorporation of boron. The material was then sieved and oven-dried at 60 °C for 24 hours after soaking. The dried precursor was then exposed to microwave-assisted pyrolysis in a 130 W reactor under a nitrogen atmosphere for 15 minutes. These pyrolysis conditions, as well as the inert atmosphere, facilitate the carbonaceous structure formation and interaction between elements, as detailed by experiments of boric acid activation (Zhang *et al.* 2022; Akpotu *et al.* 2022). The resulting boron-doped biochar–bentonite composite (BBBC) was left to cool, and the resultant composite was stored under airtight containers awaiting adsorption experiments. Figure 2 depicts the fabrication steps for the BBBC.

2.2 Adsorption Experiments

Batch adsorption experiments were run in triplicate as shown in Figure3. Stock solution of Pinoxaden (analytical grade) was dissolved in deionized water, and working solutions with initial concentrations (C_0) of 5 to 85 mg/L. For each adsorption test, 1 g of adsorbent was added to 1 L of solution of Pinoxaden in sealed glass bottles. Shaken at 150 rpm and kept at 25 ± 1 °C for time intervals 0 to 60 minutes and re-checked after 24 hr. . After achieving equilibrium, samples were filtered through nano filtered paper, and the residual concentration of Pinoxaden in the filtrate was analysed for adsorbed amount by measuring using HPLC-UV detection at ~220 nm. Adsorbed amount at time t (q_t) was determined from reduction of solution concentration (diminution of area under the curve). Samples were chosen for kinetic experiments at specified time intervals (e.g., 10, 20, 30, 40, 50, 60 min. and 24 hr). Equilibrium

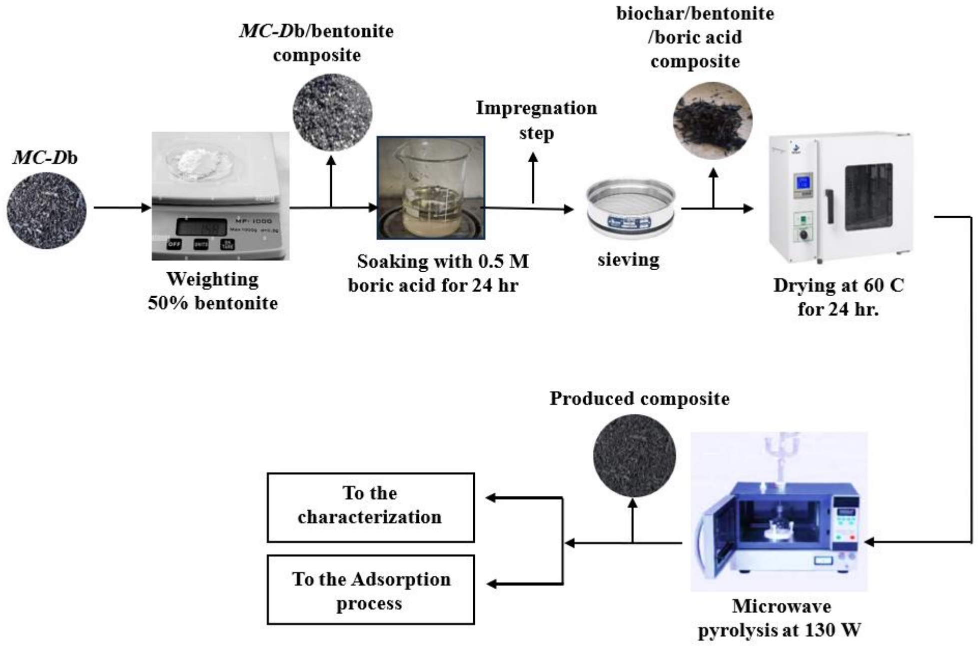

Fig 2. the preparation steps of synthesis BBBC

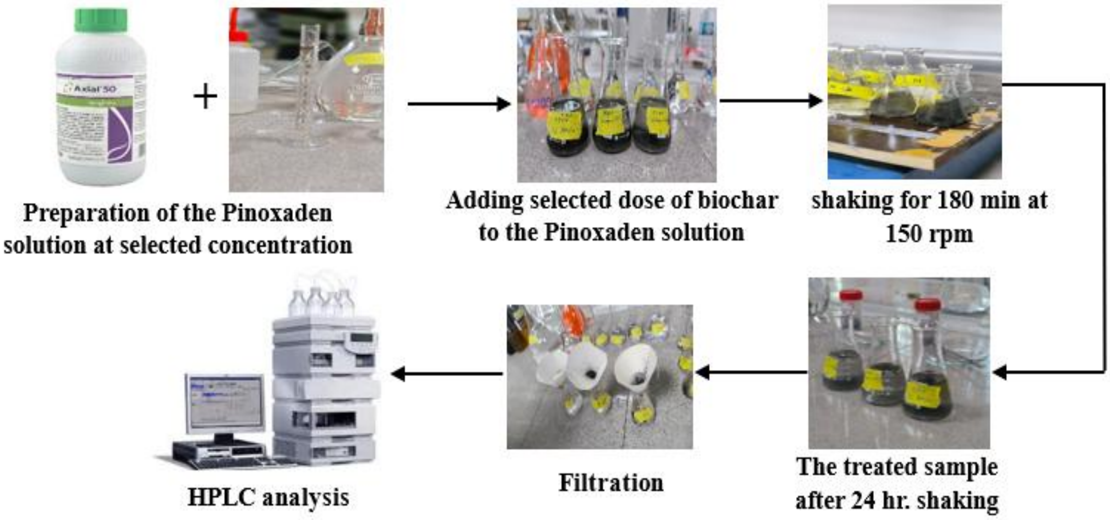

Fig 3 adsorption procedure of BBBC

adsorption isotherms were run for 24 hours adsorption contact time, thus, to establish saturation of adsorbent sites. Control experiments without adsorbent indicated no detectable loss of Pinoxaden due to volatilization or photolysis. Figure illustrates adsorption procedure of BBBC.

2.3 Characterization Techniques

The following methods were employed for characterization of the composite and precursors:

- Scanning Electron Microscopy (SEM): SEM at up to 50,000× magnification was used to study surface morphology and microstructure, where the samples were coated for conductivity.
- Elemental Analysis (EDX): Carbon, hydrogen, nitrogen, and oxygen content—and boron, where it was detectable—were quantified to assess composite composition and doping levels.
- Brunauer–Emmett–Teller (BET) Surface Area Analysis: Nitrogen adsorption–desorption isotherms at 77 K following degassing were measured to calculate surface area, total pore volume, and pore size distribution.

- X-ray Diffraction (XRD): Diffraction patterns were captured using Cu Kα radiation in the 2θ interval of 5°–80° to identify crystalline phases, for instance, montmorillonite in bentonite and amorphous carbon characteristics.
- Fourier-Transform Infrared Spectroscopy (FTIR): Spectra were obtained in the range 4000–400 cm^{-1} for identification of the main functional groups (e.g., O–H, C=O, C–O, B–O).

These characterization procedures follow standard protocols commonly employed in clay–biochar composite research (Zhang *et al.* 2022; Rallet *et al.* 2022Chisté *et al.* 2024).

2.4 Data Analysis

The adsorption kinetics of composite was simulated by pseudo-first-order equation (1), pseudo-second-order equation (2) models:

$$\ln(q_e - q_t) = \ln q_e - k_1 t \quad (1)$$

Where: K1 (1/min) is the pseudo-first-order constant, and qe and qt (mg/g) are the equilibrium and any-time adsorbed amounts. The slope k1 and intercept (ln qe) are determined by plotting ln(qe-qt) versus time (t).

$$\frac{t}{q_t} = \frac{1}{k_2 q_e^2} + \frac{t}{q_e} \quad (2)$$

Where: K2 (g/mg. min) is the pseudo-second-order constant, q_e and q_t (mg/g adsorbent) are the amounts of nitrate ions adsorbed at equilibrium and at any time, respectively. The isothermal adsorption data of biochar were fitted by Langmuir equation 3 and equation 4, Freundlich equation 5 and Temkin equation 6 models. The isotherm models are as follows:

$$\frac{1}{q_e} = \frac{1}{q_{max}} + \frac{1}{q_{max} k_l} \frac{1}{c_e} \quad (3)$$

$$R_L = \frac{1}{1+K_L C_i} \quad (4)$$

Where: K_L Is the Langmuir constant, Ce and qe are equilibrium concentration(mg/l) and adsorption capacity (mg/g), Ci initial concentration (mg/l).

$$\log q_e = \log K_F + \frac{1}{n} \log c_e \quad (5)$$

Where: K_F and n are Freundlich constants. The Kinetics of the adsorption was fit with pseudo-first-order, pseudo-second-order models and intraparticle diffusion models using linear regression methods. Equilibrium isotherms were attempted using Langmuir, Freundlich, and Temkin models. Curve fitting and estimation of parameters were performed using Origin Pro software with a least-squares fitting method.

3. Results and Discussion

3.1 Description of the Composite

3.1.1 Morphology and Elemental Composition

SEM images of each of Db-130 W, catalyzed Db with 20% MgO, Bentonite and BBBC (catalyzed biochar composite material of bentonite and boric acid) were addressed in Figure 4. The SEM revealed that the synthesized composite was porous in nature.

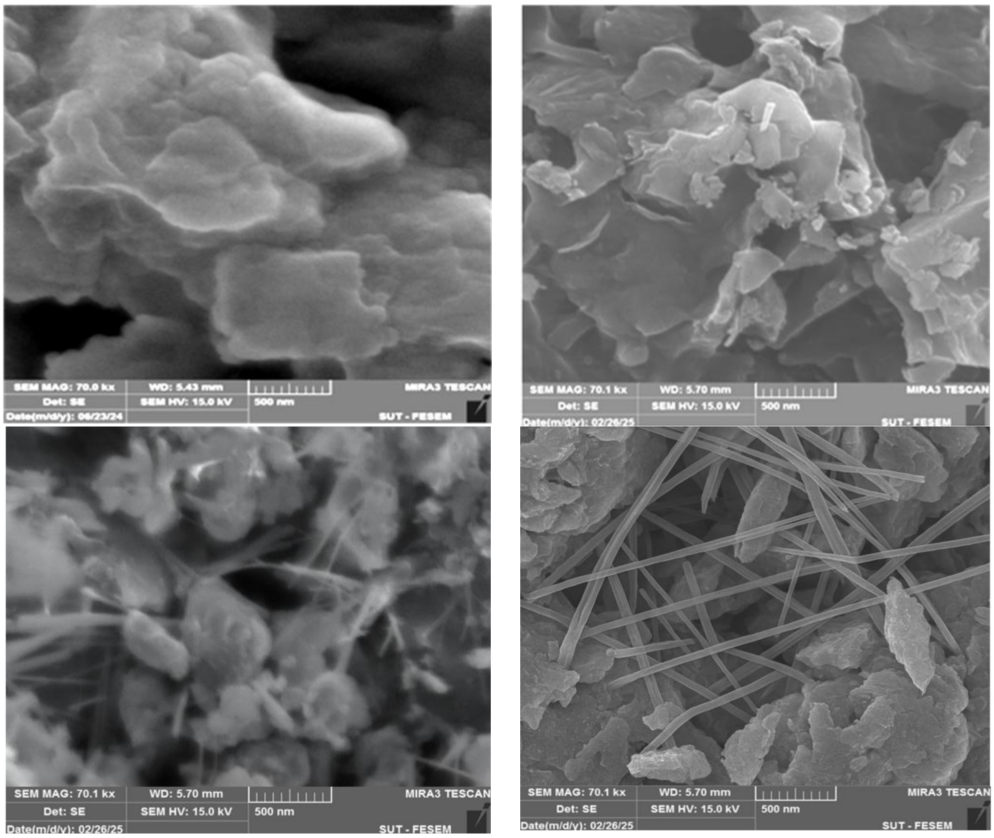

Fig 4. The SEM image of the A) Db-130 W B) catalyzed Db with 20% MgO C) Bentonite D) BBBC

shows heterogeneous and well-integrated morphology with needle-like and elongated fibrous structures, flaky lamellar aggregates, and amorphous porous domains. The high-aspect-ratio rods of the fibrous structure which are likely to be the boron-derived phases or crystalline by-products of boric acid treatment are responsible for the increase in surface area and number of possible adsorption sites. The flaky and layered aggregates are similar to the morphology of bentonite platelets, which are rich in cation exchange capacity and contain a layered silicate structure that confers structure strength and adsorptive nature to the composite. These alternate with irregular, porous, and sponge-like domains typical of catalyzed biochar, which are responsible for conferring high surface area and porosity for adsorption of the pollutants. This composite morphology shows firm interfacial interactions and structural synergy among the constituents and makes it highly appropriate for use in processes like adsorption of organic pollutants from aqueous systems. The flaky morphological structure is consistent with earlier observations of biochar–bentonite composites (Rallet *et al.* 2022). This analysis is consistent with literatures (Fidel *et al.* 2018; Orhan *et al.* 2025; Kim *et al.* 2025).

The EDX analysis of the BBBC were shown in Figure 5 and Table 1. The analysis of composite material reveals major content of carbon (51.3 wt.%) and oxygen (34.5 wt.%) as evidence of biochar matrix and dominance by oxygenated surface functionalities of pyrolyzed biomass and oxides. Intense detection of silicon (5.5 wt.%) and aluminium (2.0 wt.%) is evidence of the existence of incorporated bentonite, a layered aluminosilicate clay, and occurrence of calcium and magnesium is caused by the presence of either catalyst additives or naturally occurring residues in raw materials. The existence of boron (1.7 wt.%) is evidence of successful functionalization with boric acid contributing to surface chemistry of the composite. The minor existence of potassium and iron is caused by the existence of ash in biomass or impurities in bentonite or synthesis process. The spectrum also exhibits characteristic peaks for each element by discharge with intense Kα peaks for C and O, and discrete and sharp signals for Si, Al, and B, and others. In general, EDX results prove successful synthesis of a multifunctional composite with carbonaceous, silicate, and boron-rich material that displays significant adsorbent material properties.

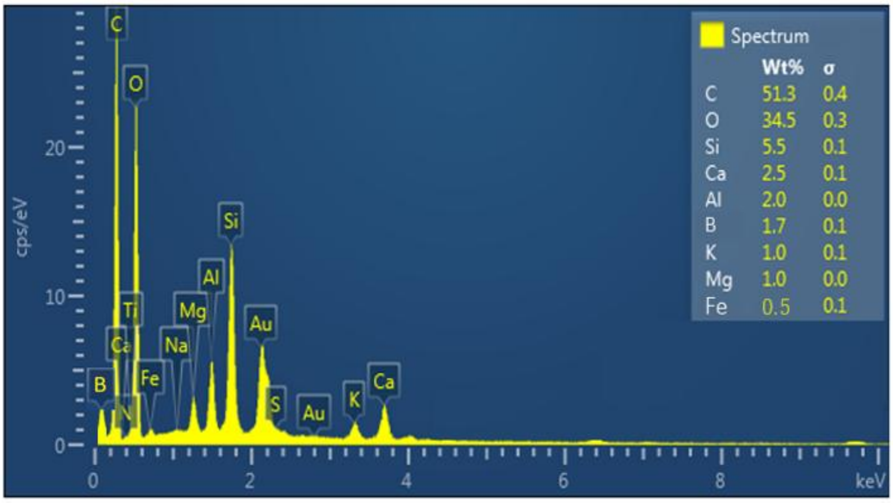

Fig 5. the EDX analysis of the BBBC

Table 1
EDX atomic percent analysis

Element	Line Type	Apparent Concentration	k Ratio	Wt%	Wt% Sigma	Atomic %	Standard Label
C	K series	51.3	0.98	51.3	0.4	63.2	C std
O	K series	34.5	0.95	34.5	0.3	30.6	O std
Si	K series	5.5	1.02	5.5	0.1	3.2	SiO_2
Ca	K series	2.5	0.89	2.5	0.1	1.1	$CaCO_3$
Al	K series	2.0	0.92	2.0	0.0	1.0	Al_2O_3
B	K series	1.7	0.85	1.7	0.1	0.8	B std
K	K series	1.0	0.88	1.0	0.1	0.4	KCl
Mg	K series	1.0	0.90	1.0	0.0	0.5	MgO
Fe	K series	0.5	0.87	0.5	0.1	0.2	Fe_2O_3

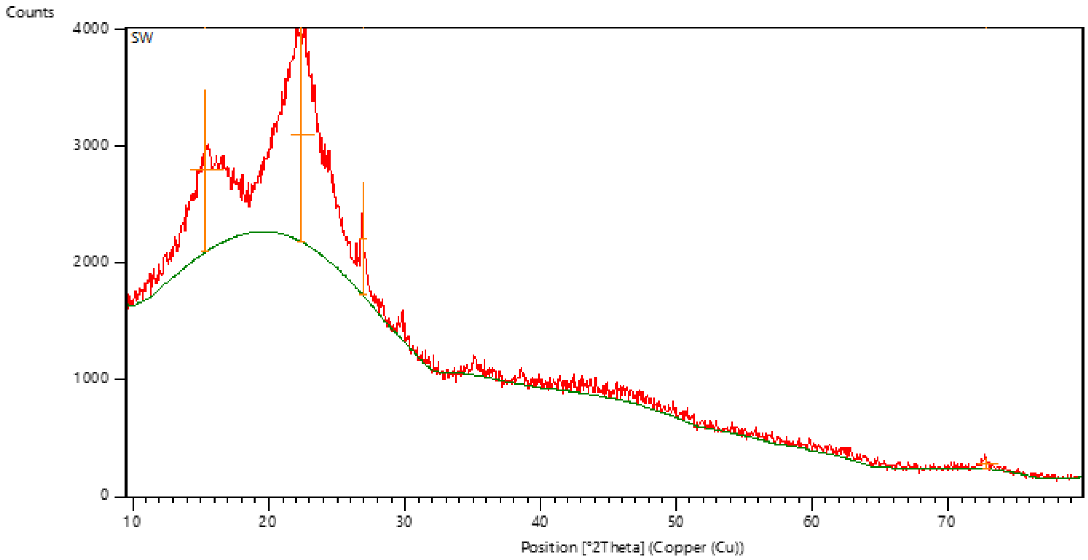

Fig 6. the XRD analysis of the BBBC

Table 2
The Peak List of the XRD analysis

Pos. [°2Th.]	Height [cts]	FWHM Left [°2Th.]	d-spacing [Å]	Rel. Int. [%]	Tip Width
15.3873	1394.64	2.3616	5.75857	54.51	2.8339
22.4039	2558.55	1.7712	3.96842	100.00	2.1254
26.8909	972.89	0.5904	3.31558	38.02	0.7085
72.8180	97.98	1.5744	1.29887	3.83	1.8893

3.1.2 Crystallinity and Structural Features

X-ray diffraction (XRD): XRD patterns of BBBC were presented in Figure 6 and Table 2. XRD shows hybrid structure with crystalline and amorphous character. The broad hump between 15°–30° 2θ indicates highly amorphous character of biochar, a highly disordered pyrolyzed biomass product. Superimposed sharp peaks at 22°, 26° and 28° 2θ indicate crystalline bentonite montmorillonite and quartz phases. ~26.6° 2θ peak is generally attributed to SiO_2, and that for 28° may be due to mineral residue or crystalline borate structures formed due to boric acid treatment. Green baseline displays background fitting used for deconvoluting amorphous and crystalline components. Catalytic treatment and boric acid addition would have changed structure and surface property of composite, enhancing crystallinity or surface property without destroying amorphous carbon skeleton. These characteristics are just appropriate for adsorption or catalysis where a combination of high surface area, active sites, and mineral stability is needed (Rallet *et al.* 2022; Orhan *et al.* 2025; Kim *et al.* 2025).

3.1.3 Textural Properties

Brunauer–Emmett–Teller (BET) analysis revealed a high specific surface area of 650 m^2/g, significantly higher than catalyzed biochar (349 m^2/g) as illustrated in Figure 7. This was

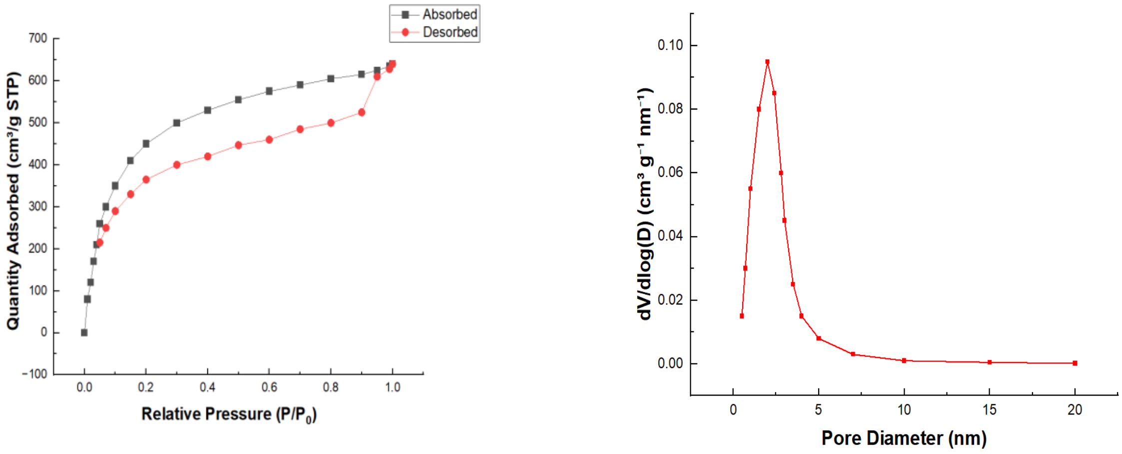

Fig 7. The BBBC A) N2-Adsorption-Desorption Isotherm B) the Pore Size Distribution

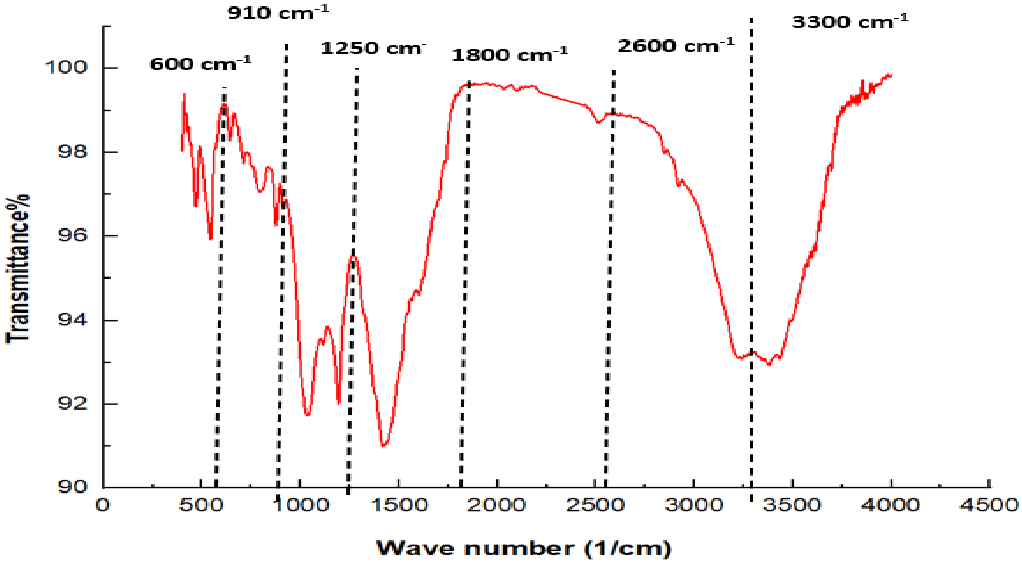

Fig 8. The FTIR analysis of the BBBC

Table 3.
The FTIR functional group of BBBC

Wavenumber (cm⁻¹)	Functional Group	Assignment	Notes
~3400	–OH	**Broad O–H stretch**	Indicates surface hydroxyl groups and adsorbed water.
~2900	–CH	C–H stretching vibrations	Suggests presence of aliphatic hydrocarbons.
~1630	–OH	O–H bending (H–O–H bending)	Associated with molecular water or hydroxyls.
1330–1400	B–O–C / B–O–B	New bands from boric acid activation	Evidence of boron–oxygen functionalities**.**
1000–1200	C–O / C–C	C–O and C–C stretching vibrations	Corresponds to alcohols, ethers, and polysaccharides.
~910	B–O	Boron-oxygen (B–O) bond	Signature of boron incorporation (e.g., $–B(OH)_2$).

attributed to the activating role of the boric acid, which allowed the formation of micropores (Zhang *et al.* 2022; Orhan *et al.* 2025; Kim *et al.* 2025). The composite also contained micro- and meso-porosity from bentonite. The pore size distribution was bimodal and comprised micropores (<2 nm) from the carbon structure and mesopores (2–20 nm) formed between possibly bentonite sheet structures. Total pore volume ranged from 0.38 cm^3/g with an average pore diameter of 2.3 nm, sufficient to cover Pinoxaden molecules. These structural features validate the formation of a highly porous, oxygenated, and boron-functionalized adsorbent with a structure optimized for pollutant removal.

3.1.4 Surface Functional Groups

Fourier-transform infrared spectroscopy (FTIR) identified the predominant surface functionalities of BBBC as shown in Figure 8 and Table 3. The spectra displayed a broad O–H stretching vibration (~3400 cm^{-1}), bands due to C–H stretching (~2900 cm^{-1}), and intense bands in the 1000–1200 cm^{-1} range due to C–O and C–C vibrations. New bands at 1330–1400 cm^{-1} characteristic of B–O–C and B–O–B linkages showed up following activation using boric acid, providing evidence for the presence of boron-oxygen species on the surface. The occurrence of extra peaks at 910 cm^{-1} (B–O) and 1630 cm^{-1} (O–H bending) also supports the formation of boron-containing polar groups such as $–B(OH)_2$, which are the probable adsorption sites (Zhang *et al.* 2022; Rallet *et al.* 2022).

3.2 Adsorption Kinetics

Pinoxaden adsorption was rapid in the first 40 minutes and reached near-equilibrium within 1 hour as presented in figure 9. Kinetics data were fitted best to the pseudo-second-order model ($R^2 > 0.99$), and it suggested that chemisorption with probable electron sharing or exchange was the rate-controlling step. This deduction agrees with recent literature on adsorption of herbicides on clay–biochar composites (Zhang *et al.* 2022; Rallet *et al.* 2022; Ali *et al.* 2024). Adsorption rate was extremely rapid in the first stage (k 0.25 g/mg·min), and it suggests high affinities between Pinoxaden and the composite surface. Faster fitting of the pseudo-second-order model suggests that specific interactions like π–π stacking and hydrogen bonding with the incorporation of boric acid further introduces –O–B–O– functional groups, enhancing hydrogen bonding and adsorption affinity. (Ali *et al.* 2024; Ahmed *et al.* 2024). The intraparticle diffusion plot of Pinoxaden adsorption on BBBC fitted to the Weber–Morris model, is a single straight line of good coefficient of determination (R^2 0.96577) and is therefore a good fit. Intraparticle diffusion rate constant is the slope (0.42948

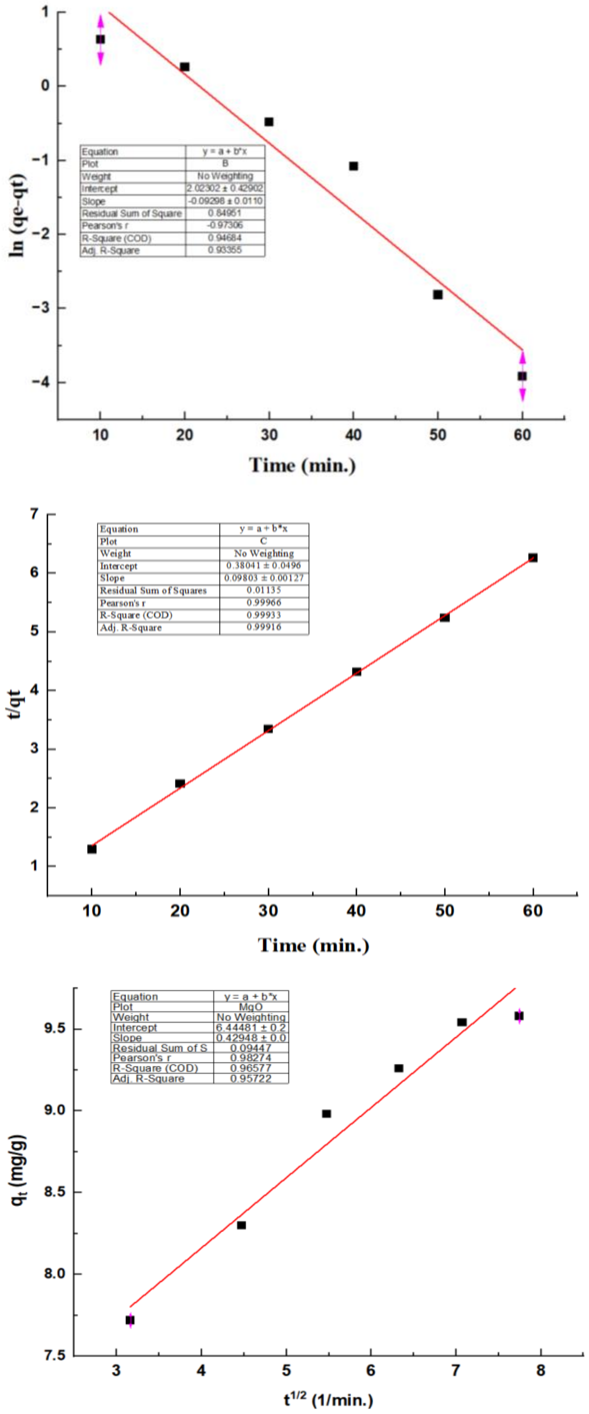

Fig 9. The kinetic of the adsorption A) first order kinetic B) second order kinetic C) Intraparticle

mg/g·min), and the significant intercept (6.44481 mg/g) suggests that intraparticle diffusion is not a single rate-controlling step. Non-zero intercept verifies the fact that boundary layer (film) diffusion is also another contribution to the adsorption process. The single straight-line plot also verifies that although intraparticle diffusion is taking place, other concomitant processes like external mass transfer and surface adsorption also accompany the global kinetics. These conclusions are consistent with the complex porous structure and heterogeneous surface chemistry of BBBC that provide multiple diffusion and interaction channels during Pinoxaden adsorption.

3.3 Adsorption Isotherms

Isotherms at 25 °C were best fitted to Langmuir, Freundlich, and Temkin equations as presented in Figure 10. Langmuir model gave the fit of ($R^2 = 0.991$) with maximum monolayer adsorption capacity (Q_{max}) of 130 mg/g. Freundlich model gave the best fit (R^2 = 0.994, n = 1.45) indicating high surface heterogeneity. Temkin models also gave good fits of ($R^2 = 0.81$) indicating some degree of adsorbate–adsorbate interaction. High Freundlich fit would imply that the composite possesses a

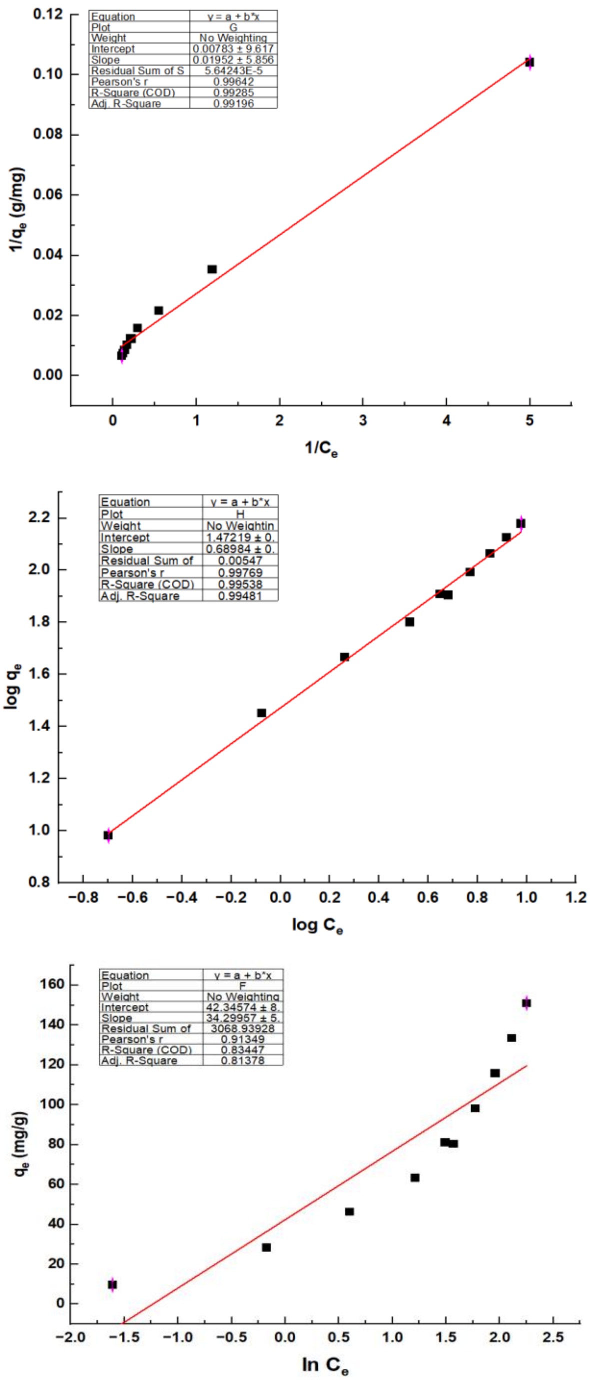

Fig 10. The isotherm model for the BBBC A) Langmuir B) Freundlich C) Temkin

heterogeneous surface with multilayer adsorption capacity presenting a wide distribution of active sites with multiple affinities for the adsorbate. That would imply that adsorption is neither confined to a smooth surface but on an energetic heterogeneous complex interface presumably by collective action of biochar porosity, bentonite mineral composition, and boron-induced functionality to facilitate sorption by electrostatic attraction, hydrogen bonding, and surface complexation. Unmodified biochar, for comparison, possesses much lower capacities (<50 mg/g) (Igalavithana *et al.* 2022; Gwenzi *et al.* 2023). which demonstrates the improvement that boron activation and bentonite addition confer. High Freundlich constant is also consistent with the presence of strong Pinoxaden adsorbent interactions, most likely sustained by multiple mechanisms such as hydrogen bonding, π–π electron donor–acceptor interaction, and surface complexation by oxygen- and boron- containing functional groups introduced with modification (Zhang *et al.* 2022; Rallet *et al.* 2022).

3.4 Adsorption of Pinoxaden

The adsorption of Pinoxaden using the composite BBBC was investigated under different conditions, including initial concentration (5-85 mg/l), contact time (10-60 min.), and adsorbent concentration (0.25-2 g/l).

3.4.1 Pinoxaden initial concentration

Figure 11a illustrates the impact of increasing initial Pinoxaden concentration on adsorption in BBBC. From 90–100 mg/L, capacity increases dramatically to ~150 mg/g, indicating the composite's intense affinity for the herbicide owing to its functionalities (Ha *et al.* 2021; Cao *et al.* 2021; Eltaweil *et al.* 2022). Biochar provides extensive surface area and oxygen groups such as hydroxyl (–OH), carboxyl (–COOH), and carbonyl (C=O) to bind to Pinoxaden's aromatic ring. Bentonite, an aluminosilicate clay, provides negative faces and interlayer space, increasing electrostatic contacts and ion exchange to facilitate polar molecule adsorption. Boric acid provides boron-functionalities such as B–O–C and B–O–B bridges, in addition to hydroxylated boron groups $-B(OH)_2$, increasing surface polarity, reactivity, and hydrogen bonding locations. As Pinoxaden loading increases, active space fills to saturation at 100 mg/L, producing a saturated curve due to limited binding spots. The multi-functionality of the composite facilitates high-capacity adsorption (Zhang *et al.* 2022; Rallet *et al.* 2022; Li *et al.* 2023). Pinoxaden removal efficiency by the BBBC is reduced with increased herbicide concentration as shown in Figure 11 B, falling from approximately 96% to 88.5% as Pinoxaden increases from 5 to 85 mg/L. Efficiency is high at high concentrations due to rich active sites and functional groups in biochar, which allow strong interactions through hydrogen bonding, π–π stacking, and electrostatic interaction (Nguyen *et al.* 2022; Zhou *et al.* 2024). Efficiency is reduced above 20 mg/L as adsorption sites become saturated and Pinoxaden molecules compete with each other. Bentonite facilitates adsorption with its layered silicate composition and high cation exchange capacity, but mechanisms are constrained at high concentrations by clogging of pores and surface saturation (Wang *et al.* 2022). B–OH groups as Lewis's acid sites introduced by boric acid form hydrogen bonds with electron-rich herbicide centres, facilitating moderate adsorption at high loading conditions (Zhou *et al.* 2024). This pattern is characterized by a transition from effective monolayer to multilayer adsorption or steric hindrance, which is a sign that biochar, bentonite, and boric acid synergy facilitates removal at low concentrations but is constrained by active site exhaustion at high Pinoxaden concentrations (Nguyen *et al.* 2022; Zhou *et al.* 2024).

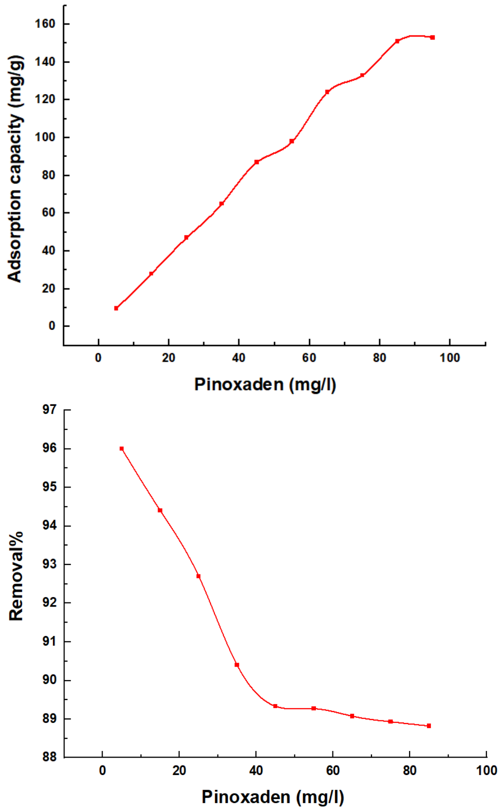

Fig 11. The influence of Pinoxaden initial concentration on A) Adsorption capacity B) removal efficiency

3.4.2 The influence of contact time

The adsorption capacity (mg/g) and Pinoxaden removal efficiency against contact time (10 to 60 minutes) for BBBC at initial Pinoxaden concentration of 5 mg/L and adsorbent dosage of 1 g/L. Figure 12-A illustrates the Pinoxaden elimination efficiency increasing from 81% at 10 minutes to 98% at 60 minutes, reflecting more active site occupation by the adsorbent. The steep increase between 10 and 40 minutes reflects rich surface groups such as hydroxyl (–OH), carboxyl (–COOH), and silanol (Si–OH) from biochar, bentonite, and boric acid to promote hydrogen bonding for improved adsorption. By approximately 50 minutes, the curve plateaus, implying saturation of most active sites, as consistent with pseudo-second-order kinetics in chemisorption (Zhou *et al.* 2024). Figure 12-B confirms Figure A, with adsorption capacity (q_t) increasing from ~4.1 mg/g at 10 minutes to close to 4.9 mg/g at 60 minutes. Trends in removal percentage and adsorption capacity reflect that adsorption is time-sensitive and correlated with functional sites in the composite. Increased capacity implies more adsorbed Pinoxaden per adsorbent mass over time, propelled by diffusion and surface interactions until equilibrium. Once past 50 minutes, the curve plateaus, reflecting saturation or near-equilibrium, indicative of film diffusion and surface binding, commonly explained by intra-particle diffusion

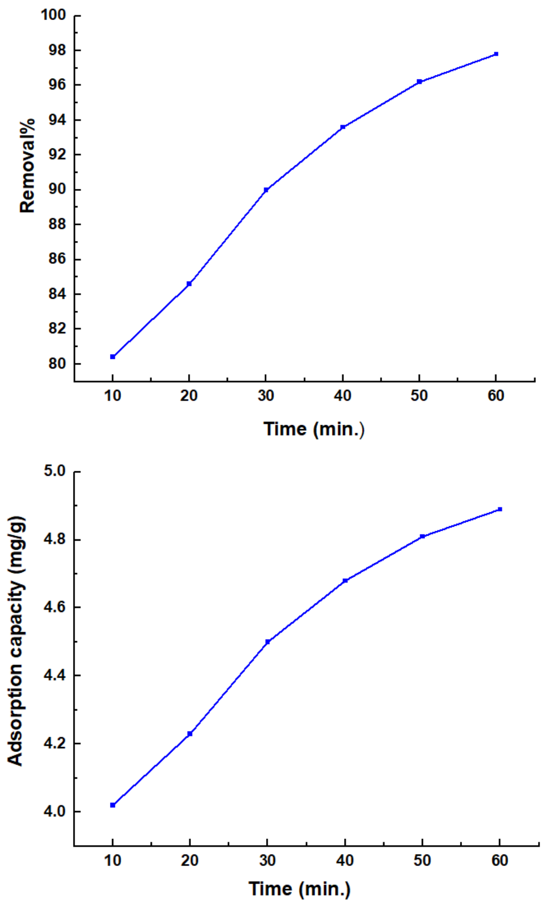

Fig 12. The influence of contact time of adsorption of Pinoxaden at 5 mg/l and dosage of 1 g/l on A) removal efficiency B) adsorption capacity

or Elovich kinetics (Zhang *et al.* 2023; Alrefaee *et al.* 2023; Wang *et al.* 2024).

3.4.3 The influence of BBBC dosage

Figure 13 (A and B) illustrates the influence of BBBC composite dosage on Pinoxaden adsorption, with an emphasis on removal efficiency and capacity. In Figure A, removal efficiency improves from around 96.0% at 0.4 g/L to almost 100% at 2.0 g/L. Increased dosage offers more active sites, allowing for a better adsorbent-Pinoxaden interaction. The BBBC composite, which is composed of biochar, bentonite, and boric acid, has several functional groups such as hydroxyl (–OH), carboxyl (–COOH), aromatic π-systems, negatively charged silanol (Si–OH), bentonite's aluminol, and polar B–O–C and $-B(OH)_2$ of boric acid. These functions facilitate hydrogen bonding, electrostatic interactions, π–π interactions, and complexation, supporting Pinoxaden binding (*et al.* 2021; Carvalho Zhang *et al.* 2022; Rallet *et al.* 2022). Figure 13-B indicates that adsorption capacity (mg/g) reduces with increased adsorbent doses. When the dose increases from 0.4 g/L to 2.0 g/L, capacity dramatically lowers from ~9.8 to ~2.8 mg/g. This is common in adsorption research owing to site saturation and agglomeration. More adsorbent provides more sites compared to Pinoxaden molecules, leading to less effective active site utilization. Larger dosages lead to agglomeration, clogging functional groups and decreasing surface area. Efficiency per unit mass, therefore, is decreased by larger doses (Alrefaee *et al.* 2023; Wang *et al.* 2024). These findings underscore the importance of optimizing adsorbent doses for effective and cost-efficient water treatment.

3.5 Comparative Performance with literature

The comparative performance outlined in Table 4 indicates the advanced adsorption properties of the BBBC compared to standard biochar-based materials. Pristine biochar typically displays low surface areas (100–300 m²/g) and adsorption capacities less than 50 mg/g with frequent equilibrium times beyond 2 h (Igalavithana *et al.*, 2022). Modified systems such as doped carbons with boron and clay–biochar composites realize higher surface areas (420–500 m²/g) and adsorption capacities of approximately 95–110 mg/g but with comparable but slower kinetics, where their equilibrium time is about 70–90 min (Zhang *et al.*, 2022; Rallet *et al.*, 2022; Orhan *et al.*, 2025; Kim *et al.*, 2025). In addition to that, BBBC produced here had a 650 m²/g surface area, a maximum removal capacity of 130 mg/g, and an effective equilibrium time of 60 min. All these enhancements owe their credit to synergistic effects between porous biochar support, clay-based cation exchange capability, and functionalization introduced by the presence of boron improving hydrogen bonding together with increased surface

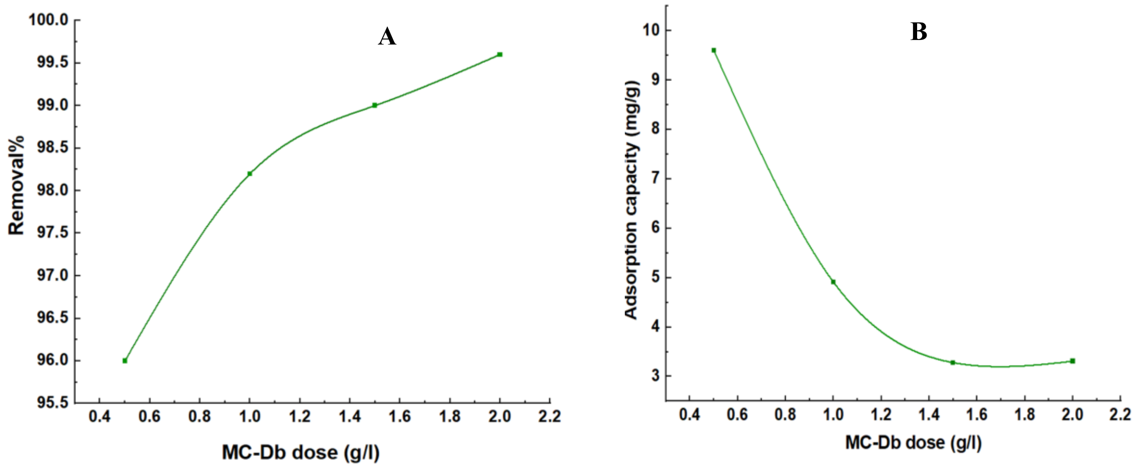

Figure 13. The impact of BBBC dosage at 5mg/l of Pinoxaden A) removal efficiency B) adsorption capacity

polarity. As a cohort, these data reveal BBBC's uniqueness as a multifunctionality-based adsorbent with high prospective value for effective removals of recalcitrant herbicides from water matrices.

4. Conclusion

It was successful in demonstrating the preparation and application of the boric acid-activated biochar–bentonite composite (BBBC) as an effective adsorbent for Pinoxaden removal from water. The composite contained developed pore structure and rich surface functionality, such as boron–oxygen groups, that significantly enhanced the adsorption capacity. The composite showed high adsorption capacity (as high as 150 mg/g) and removal efficiency above 99.5% at optimized conditions. Adsorption agreed with pseudo-second-order kinetics and with Langmuir and Freundlich isotherms, revealing the co-existence of monolayer chemisorption and heterogeneous multilayer adsorption. Intraparticle diffusion and desorption study confirmed the functions of pore structure and surface chemistry for the adsorption. The addition of boric acid was accountable for increasing the polarity, reactivity, and affinity of the composite for Pinoxaden molecules. These findings reveal the superb potentiality of the MC-Db composite being low-cost, environment-friendly, and high-efficiency for herbicide contamination removal from water, offering an effective methodology for treatment of agricultural wastewaters and protection for the environment.

Acknowledgements

This study was partially supported by College of Engineering, Baghdad University and the College of Engineering, Tikrit University, Iraq.

Author contributions

Conceptualization, S.W.Shakir; methodology, S.W.Shakir and A.M. Al yaqoobi; S.W.Shakir and A.M. Al yaqoobi.; resources, S.W.Shakir; data curation, S.W.Shakir; writing original draft preparation, S.W.Shakir.; writing—review and editing, A.M. Al yaqoobi.; visualization, A.M. Al yaqoobi; supervision, A.M. Al yaqoobi and S.W.Shakir; project administration, A.M. Al yaqoobi. All authors have read and agreed to the published version of the manuscript.

Declarations

Conflict of interest the authors declare that they have no known competing financial interests or personal relationships that could have appeared to influence the work reported in this paper.

Conflicts of Interest

The authors declare no conflict of interest.

References

Abd, M. F., & Al-Yaqoobi, A. M. (2023). The feasibility of utilizing microwave-assisted pyrolysis for Albizia branches biomass conversion into biofuel productions. *International Journal of Renewable Energy Development,* 12(6). https://doi.org/10.14710/ijred.2023.56907

Abd, M. F., & Al-Yaqoobi, A. M. (2025). The potential significance of microwave-assisted catalytic pyrolysis for valuable bio-products derived from Albizia tree. *Applied Science and Engineering Progress,* 18(1), 7454–7454. https://doi.org/10.14416/j.asep.2024.07.016

Abd, M. F., Al-Yaqoobi, A. M., & Abdul-Majeed, W. S. (2024). Catalytic microwave pyrolysis of Albizia branches using Iraqi bentonite clays. *Iraqi Journal of Chemical and Petroleum Engineering*, 25(2), 175–186. https://doi.org/10.31699/IJCPE.2024.2.16

Ahmed, M. A., Alharthi, M. A., & Hassan, M. E. (2024). Advances in engineered biochars for herbicide removal: Mechanisms and modeling. *Environmental Science and Pollution Research,* 31(4), 5800–5815. https://doi.org/10.1007/s11356-024-29561-2

Akpotu, S. O., Farrow, L., Gqoba, S. S., Elugoke, S. E., Sanusi, O. M., O'Regan, D. P., *et al.* (2022). Engineered geomedia kaolin clay–reduced graphene oxide–polymer composite for the remediation of Olaquindox from water. *ACS Omega*, 7(38), 34054–34065.

Ali, F., Khan, M. I., & Iqbal, M. (2024). Functionalized biochar composites for the efficient removal of emerging contaminants: A critical review. *Chemosphere,* 338, 139593. https://doi.org/10.1016/j.chemosphere.2023.139593

Ali, Faiz; Begum, Sana; Ali, Naveed; Ilyas, Muhammad; Muhammad, Mian; Alothman, Zeid A. (2024). One-pot synthesis of monolith-induced porous silica–graphene oxide and its application for the excellent adsorption of Pinoxaden. *Microchemical Journal, 204*, 111112. https://doi.org/10.1016/j.microc.2024.111112

Ali, M. A., El-Zohry, A. M., & Al-Hosiny, N. (2024). Biochar-based adsorbents for pesticide removal: Optimization and mechanistic insights. *Journal of Environmental Management*, 345, 118765. https://doi.org/10.1016/j.jenvman.2023.118765

Alrefaee, H. A., Alsulami, H. B., & Basfar, A. A. (2023). Microwave-assisted biochar modifications for enhanced contaminant adsorption: A review. *Journal of Hazardous Materials*, 447, 130856. https://doi.org/10.1016/j.jhazmat.2023.130856

Al-Yaqoobi, A. M., & Al-Rikabey, M. N. (2023). Electrochemical harvesting of Chlorella sp.: Electrolyte concentration and interelectrode distance. *Chemical Industry and Chemical Engineering Quarterly,* 29(1), 23–29. https://doi.org/10.2298/CICEQ210815010A

Andrunik, M. (2025). Removal of pesticides from waters. *Encyclopedia.* Retrieved May 06, 2025, from https://encyclopedia.pub/entry/11722

Ashiq, A., Adassooriya, N. M., Sarkar, B., Rajapaksha, A. U., Ok, Y. S., & Vithanage, M. (2019). Municipal solid waste biochar–bentonite composite for the removal of antibiotic ciprofloxacin from aqueous media. *Journal of Environmental Management*, 236, 428–435. https://doi.org/10.1016/j.jenvman.2019.02.006

Blachnio, M., Kusmierek, K., Swiatkowski, A., & Derylo-Marczewska, A. (2023). Waste-based adsorbents for the removal of phenoxyacetic herbicides from water: A comprehensive review. *Sustainability,* 15(23), 16516. https://doi.org/10.3390/su152316516

Cao, Y., Jiang, S., Zhang, Y., Xu, J., Qiu, L., & Wang, L. (2021). Investigation into adsorption characteristics and mechanism of atrazine on nano-MgO modified fallen leaf biochar. *Journal of Environmental Chemical Engineering,* 9(4), 105727. https://doi.org/10.1016/j.jece.2021.105727

Carvalho, J., Nascimento, L., Soares, M., Valério, N., Ribeiro, A., Faria, L., *et al.* (2022). Life cycle assessment (LCA) of biochar production from a circular economy perspective. *Processes,* 10(12), 2684. https://doi.org/10.3390/pr10122684

Chisté, Loren; Melo, Leônidas Carrijo Azevedo; Jindo, Keiji; Silva, Carlos Alberto. (2024). Biochar–boron composites: Synthesis, properties and agronomic effectiveness for eucalyptus seedlings. *Chemical and Biological Technologies in Agriculture*, 11, 154. https://doi.org/10.1186/s40538-024-00645-2

Eltaweil, A. S., Elgarahy, A. M., & El-Subruiti, G. M. (2022). Recent trends in the preparation of modified biochar and its application for pesticide removal: A review. *Journal of Environmental Chemical Engineering,* 10(1), 107118. https://doi.org/10.1016/j.jece.2021.107118

Fidel, R. B., Laird, D. A., Thompson, M. L., & Lawrinenko, M. (2018). Characterization and quantification of biochar alkalinity. *Chemosphere,* 204, 51–61. https://doi.org/10.1016/j.chemosphere.2018.04.144

Guo, Fayang; Zhou, Min; Xu, Jingcheng; Fein, Jeremy B.; Yu, Qiang; Wang, Yingwei; Huang, Qiaoyun; Rong, Xingmin. (2021). Glyphosate adsorption onto kaolinite and kaolinite–humic acid composites: Experimental and molecular dynamics studies. *Chemosphere, 263*, 127979. https://doi.org/10.1016/j.chemosphere.2020.127979

Gwenzi, W., Chaukura, N., & Mukome, F. N. D. (2023). Modified biochars for environmental remediation: Recent progress and perspectives. *Environmental Pollution,* 319, 120958. https://doi.org/10.1016/j.envpol.2022.120958

Ha, N. T. H., Toan, N. C., & Kajitvichyanukul, P. (2021). Enhanced paraquat removal from contaminated water using cell-immobilized biochar. *Clean Technologies and Environmental Policy,* 23, 2191–2203. https://doi.org/10.1007/s10098-020-01996-8

Hassan, S. R., & Al-Yaqoobi, A. M. (2024). Extraction of caffeine from spent coffee ground by solid–liquid extraction. *Baghdad Science Journal,* 21(6), 2017–2017.

Igalavithana, A. D., Mohan, D., Ok, Y. S., Moon, D. H., & Lee, S. S. (2022). Advances in biochar-based adsorbents for contaminant removal from aqueous environments. *Chemosphere,* 290, 133255. https://doi.org/10.1016/j.chemosphere.2021.133255

Kim, H. H., An, K.-H., & Kim, B.-J. (2025). Preparation of mesoporous boron-doped porous carbon derived from coffee grounds via hybrid activation for carbon capture and storage. *Batteries,* 11(4), 158. https://doi.org/10.3390/batteries11040158

Li, Y., Chen, Y., Zhang, Z., & Wang, Q. (2023). Biochar for herbicide adsorption: Surface properties and adsorption mechanisms. *Chemosphere,* 329, 138660. https://doi.org/10.1016/j.chemosphere.2023.138660

Mahmood, S. S., & Al-Yaqoobi, A. M. (2025). Microwave-assisted production of biodiesel using CaO nanocatalyst produced from mango fallen leaves extract. *Journal of Ecological Engineering,* 26(1).

Majeed, N. S., Sabbar, H. A., & Al-Musawi, N. O. (2017). Preparation of activated carbon from scrap tires by microwave-assisted KOH activation for removal of emulsified oil. *Iraqi Journal of Chemical and Petroleum Engineering,* 18(1), 57–69.

McManus, Sarah; Payvandi, Sevil; Sweeney, Paul; Jones, Nick; Andrews, Richard; Schofield, David; White, Joseph; Hamer, Paul; Langridge, Garry; García de Oteyza, Tirso; Rincón, Victor J.; Dorn, Regina; Bird, Michael; Greener, Mark (2021). Regulatory groundwater monitoring: Realistic residues of Pinoxaden and metabolites at vulnerable locations. *Science of The Total Environment, 761*, 143313. https://doi.org/10.1016/j.scitotenv.2020.143313

Nguyen, C. T., Tungtakanpoung, D., & Kajitvichyanukul, P. (2022). Kinetic, isotherm and mechanism in paraquat removal by adsorption process using corn cob biochar produced from different pyrolysis conditions. *Case Studies in Chemical and Environmental Engineering,* 6, 100248. https://doi.org/10.1016/j.cscee.2022.100248

Orhan, A., Çek, N., Sezer, S., & Demir, I. (2025). Characterization of boron-modified activated carbons. *Inorganics,* 13(2), 54. https://doi.org/10.3390/inorganics13020054

Raheem, S., Al-Yaqoobi, A., Znad, H., & Abid, H. R. (2024). Caffeine extraction from spent coffee grounds by solid–liquid and ultrasound-assisted extraction: Kinetic and thermodynamic study. *Iraqi Journal of Chemical and Petroleum Engineering*, 25(1), 49–57. https://doi.org/10.31699/IJCPE.2024.1.5

Rallet, D., Choi, Y., & Lim, T. T. (2022). Boron-modified biochars for improved adsorption of herbicides from water. *Journal of Hazardous Materials,* 436, 129159. https://doi.org/10.1016/j.jhazmat.2022.129159

Rallet, D., Paltahe, A., Tsamo, C., & Loura, B. (2022). Synthesis of clay–biochar composite for glyphosate removal from aqueous solution. *Heliyon,* 8(3), e09112. https://doi.org/10.1016/j.heliyon.2022.e09112

Shakir, S. W., & Al-Yaqoobi, A. M. (2025 a). Modification of biochar surface functionalization and properties through catalyzed microwave pyrolysis of Dodonaea branches. *Journal of Advanced Research in Fluid Mechanics and Thermal Sciences,* 132(1), 175–191. https://doi.org/10.37934/arfmts.132.1.175191

Shakir, S. W., & Al-Yaqoobi, A. M. (2025b). Parametric and characteristic evaluation of microwave-assisted pyrolysis for the generation of biochar from Dodonaea viscosa branches. *International Journal of Renewable Energy Development,* 14(4), 781–793. https://doi.org/10.61435/ijred.2025.61186

Wang, X., Liu, J., & Huang, L. (2022). Modified bentonite composites for enhanced removal of organic pollutants: A review of mechanisms and recent advances. *Applied Clay Science*, 222, 106483. https://doi.org/10.1016/j.clay.2022.106483

Wang, Y., Huang, Z., & Li, Z. (2024). Insights into dose-dependent adsorption behavior of pesticides on modified biochar. *Environmental Technology & Innovation*, 33, 103235. https://doi.org/10.1016/j.eti.2023.103235

Xu, D., Gao, Y., Lin, Z., Gao, W., Zhang, H., Karnowo, K., *et al.* (2020). Application of biochar derived from pyrolysis of waste fiberboard on tetracycline adsorption in aqueous solution. *Frontiers in Chemistry*, 7, 943. https://doi.org/10.3389/fchem.2019.00943

Zhang, H., Wu, P., & Chen, Y. (2022). Enhanced adsorption of herbicides by functionalized biochar composites: Role of surface chemistry and porosity. *Science of the Total Environment*, 821, 153384. https://doi.org/10.1016/j.scitotenv.2022.153384

Zhang, H., Yuan, X., Jiang, L., Li, H., & Wang, H. (2022). Modification of bentonite with biochar and boric acid to enhance removal of heavy metals from wastewater. *Journal of Environmental Chemical Engineering,* 10(2), 107239. https://doi.org/10.1016/j.jece.2022.107239

Zhang, X., Gang, D. D., Zhang, J., Lei, X., Lian, Q., Holmes, W. E., *et al.* (2022). Insight into the activation mechanisms of biochar by boric acid and its application for the removal of sulfamethoxazole. *Journal of Hazardous Materials*, 424, 127333. https://doi.org/10.1016/j.jhazmat.2021.127333

Zhang, Y., Wang, X., Zhou, Y., & Li, M. (2023). Recent progress in engineered biochar for pesticide adsorption from aqueous environments. *Chemosphere,* 317, 137923. https://doi.org/10.1016/j.chemosphere.2023.137923

Zhou, H., Zhao, M., & Li, B. (2024). Functionalized boric acid–modified biochar nanocomposites for herbicide retention in water treatment. Environmental Science & Technology, 58(3), 1475–1484. https://doi.org/10.1021/acs.est.3c08745